

Modeling Local Order in Bacterial Collective Motions

Alexander Zhu

Under the Mentorship of Boya Song
MIT Mathematics Department

Research Science Institute
July 30, 2019

Abstract

In our study, we modify an existing dynamic model of how the position and orientation of cells change as a result of their self-propulsion speed and cell-cell repulsion forces. We add a force between endpoints to create smectic alignment in the simulations in addition to nematic alignment. We use a MATLAB code to run simulations of different scenarios of cell interactions to test our improved model. Our modified model succeeds in creating smectic alignment in the two cell scenario when the cells are aligned in the same direction and when two cells are oppositely oriented with low velocities. In the 10 cell scenario, our model succeeds in creating smectic alignment when the cells have the same orientation and velocity, and they create rafts among other cells with similar speeds and orientation. We simulate scenarios with 50 cells with random orientations and positions, and our model succeeds in creating curved and linear endpoint alignment in these scenarios. Our model generates endpoint alignment when the cells have similar orientations and velocities, creating rafts similar to those seen in previous experiments.

Summary

In our study, we examine an existing model about how cells in high-density areas affect one another. The changes in position and orientation, which is the direction the cell is pointing, depend on the speed of the cells, the direction of the cells, and the repulsive forces that the cells force on each other. We modify the model to generate more endpoint alignment, which is when the endpoints of the cells lie in a straight line. We also create orientational alignment. Our model succeeds in creating this type of alignment in 2 cell, 10 cell, and 50 cell scenarios. In the 2 cell scenarios, our model creates alignment for the cases where the cells are moving in the same direction or when they move at a speed of 0. In the 10 cell scenarios, the simulations from the model show that cells with similar orientations and speeds group together and move with endpoint alignment. In the 50 cell scenarios, the cells move with random speeds and orientations and still gained endpoint alignment, demonstrating the effectiveness of our model.

1 Introduction

Cells present in tissues and swarms often perform a type of self-organization. As cells move across surfaces, they swarm together to create rafts, which are groups of cells aligned with each other. The two different alignments of these swarms that have been observed in experiments are the nematic alignment and the smectic alignment [1, 2]. The nematic alignment has orientationally aligned cells without much endpoint alignment, while the smectic alignment has endpoint alignment as seen in Figure 1C. Two examples of biological systems with such alignments are shown in Figures 1A and 1B.

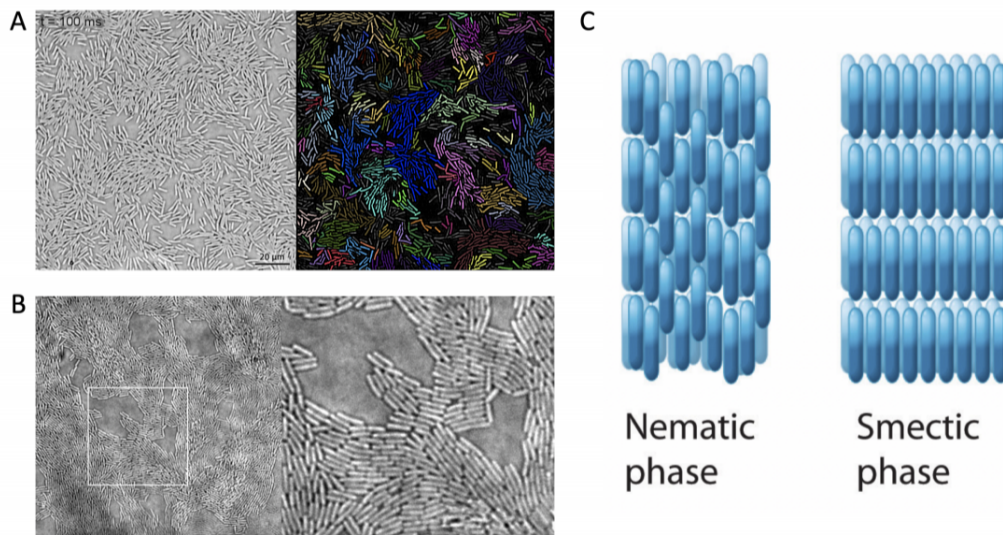


Figure 1: **A** Experimental (left) and simulation (right) snapshots of *B. subtilis* cells in the rafting phase [1]. **B** *P. aeruginosa* moving along a surface via twitching [2]. **C** The two different alignments in liquid crystal literature: nematic and smectic [3].

In their study, Jeckel et al. [1] analyzed the cell density, cell speed, fraction of cells in nonmotile clusters, and the fraction of cells in motile rafts of *B. subtilis* cells in nematic alignments. They observed the bacterial colony expand radially in an agar plate and used a microscope to capture movies of bacteria at various locations on the plate throughout the expansion of the colony. Using the data collected from high-speed microscopy and analyzed

by machine learning, the study demonstrated the five different dynamic phases of the cell swarming. From each video, Jeckel et al. [1] computed how various observables (e.g. cell speed, average raft sizes, cell density) changed over time. Based on these observables, the videos were categorized into five different phases. The study discovered clear differences among the different phases of swarming, with differences in cell speeds as seen in Figure 2 along with differences in the fraction of cells within clusters and the fraction of rafting cells. Despite the variations among the phases, a universal physical model was able to replicate all phases in simulations given the corresponding initial conditions. While the study performed by Jeckel et al. [1] was about two-dimensional cell alignment, Hartman et al. [4] studied dimensional order and structure in three-dimensional biofilms. In a manner similar to that of the two-dimensional alignment, the biofilm order arose from mechanical cell-cell interactions.

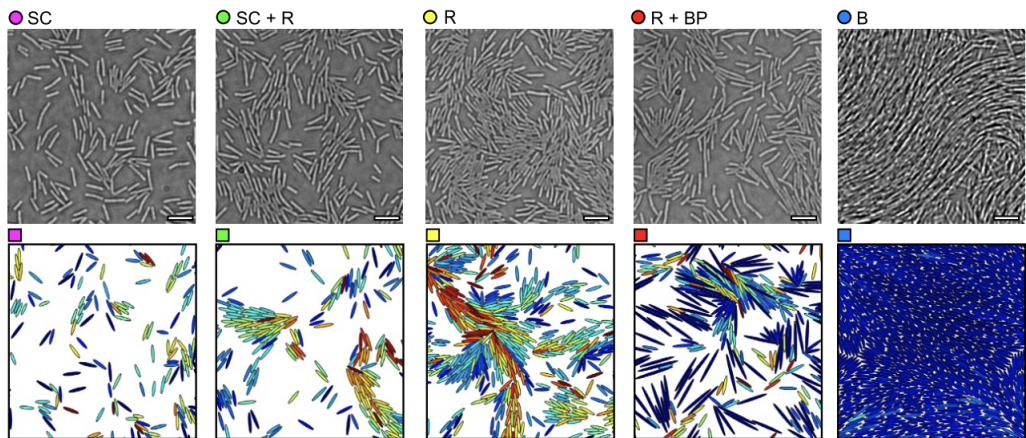


Figure 2: The five phases of swarming discovered in the experiment by Jeckel et al. [1], with the experimental snapshots on the upper row and the simulation on the lower row. In order from left to right, they are low-density single-cell (SC), single-cell and rafts (SC+R), high density rafting (R), rafts and biofilm precursors (R+BP), and biofilm (B) [1]. The different colored cells represent different cell speeds, with red cells being the fastest and blue cells being the slowest.

The agreement between simulations and the experimental observations implied that cell-cell repulsion forces and motility were enough to explain the nematic alignment in the rafts. Our study focuses on modifying the two dynamic equations describing \mathbf{x}_α , the position of

cell α , and $\hat{\mathbf{n}}_\alpha$, the orientation of cell α . The equations are the following:

$$\frac{d\mathbf{x}_\alpha}{dt} = v_\alpha \hat{\mathbf{n}}_\alpha + \Gamma^{-1} \mathbf{F}_{\text{cell-cell}} \quad (1)$$

$$\frac{d\hat{\mathbf{n}}_\alpha}{dt} = (I - \hat{\mathbf{n}}_\alpha \hat{\mathbf{n}}_\alpha^\top) (\Omega^{-1} \mathbf{T}_{\text{cell-cell}}). \quad (2)$$

Here v_α is the self-propulsion speed of the cell, which is a measured property from experiments. In Jeckel et al. [1], $\mathbf{F}_{\text{cell-cell}} = -\frac{\partial V_\alpha}{\partial \mathbf{x}_\alpha}$ in Equation (1), and $\mathbf{T}_{\text{cell-cell}} = -\frac{\partial V_\alpha}{\partial \hat{\mathbf{n}}_\alpha}$ in Equation (2), where V_α is the total cell-cell interaction potential energy for the cell α .

In Equations (1) and (2), Γ and Ω are resistance matrices described by

$$\Gamma = \gamma_0 [\gamma_{\parallel} (\hat{\mathbf{n}}_\alpha \hat{\mathbf{n}}_\alpha^\top) + \gamma_{\perp} (I - \hat{\mathbf{n}}_\alpha \hat{\mathbf{n}}_\alpha^\top)],$$

$$\Omega = \omega I.$$

Here γ_0 is the translational friction coefficient, and ω is the rotational friction coefficient. Also, γ_{\parallel} and γ_{\perp} are dimensionless parameters which characterize the longitudinal and transverse friction parameters respectively based on the aspect ratio ℓ_α/r_α , where ℓ_α is the half-length of cell α and r_α is the half-width of cell α [1].

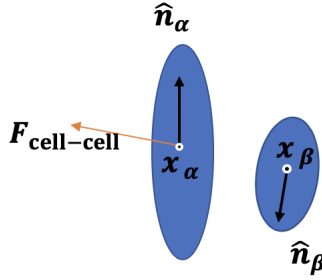


Figure 3: A diagram of two cells α and β , showing $\hat{\mathbf{n}}_\alpha$, $\hat{\mathbf{n}}_\beta$, \mathbf{x}_α , \mathbf{x}_β and $\mathbf{F}_{\text{cell-cell}}$ used in Equation (1). Here $\mathbf{F}_{\text{cell-cell}}$ is on the line connecting \mathbf{x}_α and \mathbf{x}_β .

Equation (1) describes how the position of a single bacteria cell changes with time, which is its velocity. Here $v_\alpha \hat{\mathbf{n}}_\alpha$ is how the cell moves in the direction of its orientation at the constant self-propulsion speed. Also, $\Gamma^{-1} \mathbf{F}_{\text{cell-cell}}$ describes the effects on cell positions caused by cell-cell interactions. From Jeckel et al., we have $\mathbf{F}_{\text{cell-cell}} = -\frac{\partial V_\alpha}{\partial \mathbf{x}_\alpha}$, which models how the cells move to reach their minimum cell-cell potential from repulsion forces [1]. The study

performed by Jeckel et al. considered the system to be over-damped, so we also consider our system to be over-damped. Therefore, the forces do not cause an acceleration change but change the velocities instantaneously.

In Equation (2) of our model, $\frac{d\hat{\mathbf{n}}_\alpha}{dt}$ demonstrates how the orientation of the cell changes, which is how the cell rotates with time. Here, $I - \hat{\mathbf{n}}_\alpha \hat{\mathbf{n}}_\alpha^\top$ is a matrix which converts the latter half of the equation into a vector perpendicular to $\hat{\mathbf{n}}_\alpha$. $\Omega^{-1} \mathbf{T}_{\text{cell-cell}}$ describes how the orientation of the cell changes as a result of the cell-cell interactions in Equation (2). We consider this to be similar to a torque caused by the cell-cell interactions because of the perpendicular cell-cell interaction forces involved.

We test different initial conditions and find new terms to add to $\mathbf{F}_{\text{cell-cell}}$ and $\mathbf{T}_{\text{cell-cell}}$ to adjust the cell-cell interaction forces and torques to generate more endpoint alignment and smectic alignment. We hope to gain smectic alignment in our simulations to explain the smectic order observed in experiments and to draw a connection between bacterial swarming and liquid crystal literature. We first describe how we generate simulations for our model. Then, we introduce our changes to the previous model and how our terms affect the simulations. Lastly, we discuss the results of our simulations as well as possible future work.

2 Methods

To model the bacteria, we used MATLAB to simulate the cell-cell interactions with Equations (1) and (2) and test our added forces. In our model, we used periodic boundary conditions, which allowed us to simulate an infinite system in a finite domain. The center of our system had coordinates of (0,0), with the x and y coordinates ranging from $-L$ to L . We set the periodic boundary conditions when computing the vector between two endpoints. Whenever cell α with position \mathbf{x}_α reaches the top of our boundary and vice versa, because of the periodic boundary conditions it is transported to the bottom of the system. Similarly,

when \mathbf{x}_α reaches the left side of our boundary, it is transported to the right side of our system and vice versa. Our vector is greatly changed if we ignore the periodic boundary conditions, as the vector from the endpoint of cell α to the endpoint of cell β changes from a near horizontal vector to a vertical vector or vice versa. To counteract this issue, we consider when $x \geq L$, where x is the x -coordinate of \mathbf{x}_α . When $x \geq L$, we transport the cell from this x to $x - 2L$, so that the new x -coordinate is within the boundaries of L and $-L$. Similarly, when $x < -L$, then we transport x to $x + 2L$. We also label y as the y -coordinate of \mathbf{x}_α . Then, when $y \geq L$, we transport y to $y - 2L$; when $y < -L$, we transport y to $y + 2L$. This transformation keeps the cells within the boundaries while also keeping the vectors connecting endpoints from changing dramatically when crossing boundaries. In our simulations, we used $L = 15$, corresponding to a length of 7.5 micrometers. In each figure, the cells in their initial positions and orientations are blue, while the cells in their final positions are orange.

2.1 The Endpoint Interaction Force

We design the following force to act on cell α for every pair of cells in the simulation:

$$\mathbf{F}_{\text{cell-cell}} = -K_r \frac{\partial V_\alpha}{\partial \mathbf{x}_\alpha} - K_e \frac{1}{d^3 + 1} \hat{\mathbf{n}}_\alpha^\top \cdot \mathbf{v} \quad (3)$$

Here $-\frac{\partial V_\alpha}{\partial \mathbf{x}_\alpha}$ is the cell-cell repulsion from Jeckel et al. [1]. K_r denotes the strength of the force caused by cell-cell repulsion, and K_e denotes the strength of the endpoint interaction force. We have $\hat{\mathbf{n}}_\alpha$ as the orientation of cell α . Also, ℓ_α and \mathbf{x}_α are the half-length and position of cell α , respectively. We take the dot product between $\hat{\mathbf{n}}_\alpha$ and \mathbf{v} , where \mathbf{v} is the vector connecting the pair of two endpoints to be aligned. Here $d = \|\mathbf{v}\|$ is the distance between the two endpoints which we align. We choose the decay factor to be $\frac{1}{d^3+1}$. We choose this decay factor so that the endpoint interaction force is greater for two cells that are close to each other. We also want cells that are a large distance from each other to have a negligible effect on each other. We cannot let the decay factor be $\frac{1}{d^3}$ or the force will be undefined when the cells overlap, so we make the factor $\frac{1}{d^3+1}$. To test the effectiveness of our distance

decay factor, we run a simulation of two cells whose endpoints lie a large distance apart. In Figure 4, we see that when the closest endpoints lie at a distance of 15 units apart, then the interaction force between the two cells is insignificant and does not create any endpoint alignment. This allows us to validate our model, as the cells do not align when they are far apart, but we notice that they do align when close.

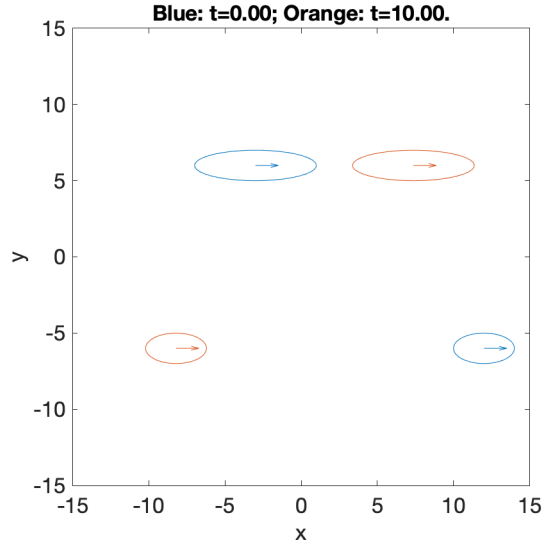


Figure 4: For two cells which have their endpoints a large distance apart, the endpoint interaction force between them has a minimal effect. The two cells do not become much closer to achieving endpoint alignment.

Before we can calculate our $\mathbf{F}_{\text{cell-cell}}$, we first choose which endpoints should align. We define four vectors, \mathbf{v}_{pp} , \mathbf{v}_{pm} , \mathbf{v}_{mp} , \mathbf{v}_{mm} such that

$$\begin{aligned}\mathbf{v}_{\text{pp}} &= \mathbf{x}_\alpha + \ell_\alpha \hat{\mathbf{n}}_\alpha - (\mathbf{x}_\beta + \ell_\beta \hat{\mathbf{n}}_\beta), \\ \mathbf{v}_{\text{pm}} &= \mathbf{x}_\alpha + \ell_\alpha \hat{\mathbf{n}}_\alpha - (\mathbf{x}_\beta - \ell_\beta \hat{\mathbf{n}}_\beta), \\ \mathbf{v}_{\text{mp}} &= \mathbf{x}_\alpha - \ell_\alpha \hat{\mathbf{n}}_\alpha - (\mathbf{x}_\beta + \ell_\beta \hat{\mathbf{n}}_\beta), \\ \mathbf{v}_{\text{mm}} &= \mathbf{x}_\alpha - \ell_\alpha \hat{\mathbf{n}}_\alpha - (\mathbf{x}_\beta - \ell_\beta \hat{\mathbf{n}}_\beta).\end{aligned}$$

Here, \mathbf{v}_{pp} is the vector connecting the endpoint of cell α in the direction of $\hat{\mathbf{n}}_\alpha$ with the endpoint of cell β in the direction of $\hat{\mathbf{n}}_\beta$ as seen in Figure 5. In a similar way, \mathbf{v}_{pm} , \mathbf{v}_{mp} , and \mathbf{v}_{mm} connect the positive endpoint of cell α to the negative endpoint of cell β , the negative

endpoint of cell α to the positive endpoint of cell β , and the negative endpoint of cell α to the negative endpoint of cell β , respectively.

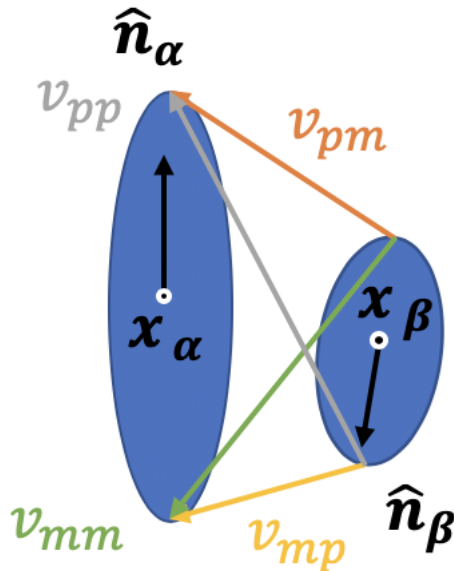


Figure 5: Two cells, with cell α on the left and cell β on the right, with each of the four vectors which we consider. The black lines are $\hat{\mathbf{n}}_\alpha$ and $\hat{\mathbf{n}}_\beta$, \mathbf{v}_{pp} is the gray vector, \mathbf{v}_{pm} is the orange vector, \mathbf{v}_{mp} is the yellow vector, and \mathbf{v}_{mm} is the green vector.

We choose \mathbf{v} to be the vector which is closest to the perpendicular with $\hat{\mathbf{n}}_\alpha$ among these four vectors. To do so, we take the dot product between $\hat{\mathbf{n}}_\alpha$ and each of the four vectors \mathbf{v}_{pp} , \mathbf{v}_{pm} , \mathbf{v}_{mp} , \mathbf{v}_{mm} . From these four dot products, we then choose the dot product with the least absolute value. We define the vector involved in that dot product as \mathbf{v} . Once we have that dot product, we can substitute it into Equation (3) to determine our $\mathbf{F}_{\text{cell-cell}}$.

In the next section, we will analyze different scenarios in simulations to show that our endpoint interaction force works as expected.

3 Results

3.1 Two Cell Scenarios

3.1.1 Two Cell Scenario with Orientational Alignment

To create more endpoint alignment, we first consider a scenario with two cells, α and β that are orientationally aligned, meaning that

$$\hat{\mathbf{n}}_\alpha = \hat{\mathbf{n}}_\beta.$$

The force we introduced in Equation (3) should satisfy the condition that it is nonzero when the two cells do not have endpoint alignment and is zero when the two cells have endpoint alignment. In the two cell scenarios in Figure 6, there are no other cells which apply a force on cell α , so cell α only has one endpoint interaction force acting on it. In Figure 6A, we can simplify Equation (3) to

$$\mathbf{F}_{\text{cell-cell}} = -K_r \frac{\partial V_\alpha}{\partial \mathbf{x}_\alpha} - K_e \frac{1}{d^3 + 1} \hat{\mathbf{n}}_\alpha^\top \cdot (\mathbf{x}_\alpha + \ell_\alpha \hat{\mathbf{n}}_\alpha - (\mathbf{x}_\beta + \ell_\beta \hat{\mathbf{n}}_\beta)).$$

Our $\mathbf{F}_{\text{cell-cell}}$ is proportional to the dot product between $\hat{\mathbf{n}}_\alpha$ and $\mathbf{x}_\alpha + \ell_\alpha \hat{\mathbf{n}}_\alpha - (\mathbf{x}_\beta + \ell_\beta \hat{\mathbf{n}}_\beta)$, which is the vector connecting the two positive endpoints of cell α and β . We choose the two positive endpoints to create our vector \mathbf{v} because the two cells are oriented in the same direction. When endpoint alignment occurs, the dot product becomes 0, and the force also becomes 0. After fixing this condition, our simulations succeed in creating endpoint alignment throughout the boundaries in the two cell scenario with orientational alignment, as seen in Figure 6A. This $\mathbf{F}_{\text{cell-cell}}$ works to create endpoint alignment for a two cell system. However, when we create this $\mathbf{F}_{\text{cell-cell}}$, we also assume that the cells have the same orientation.

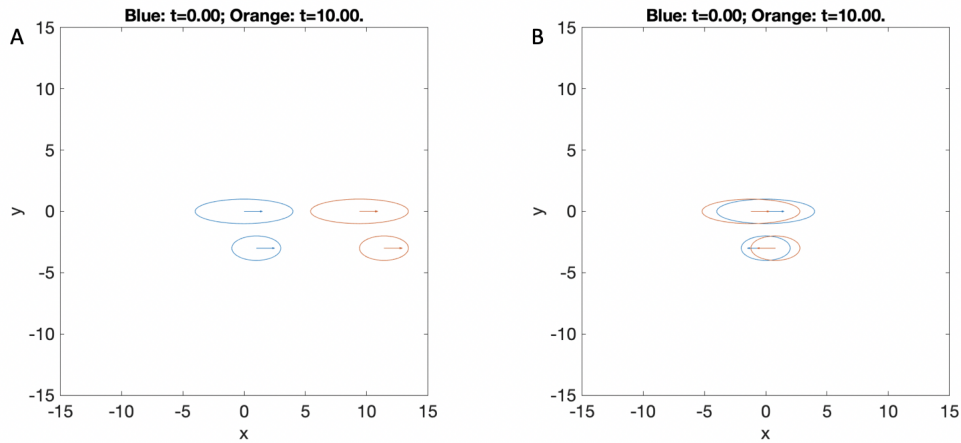


Figure 6: **A** We have two cells with the same orientation and the same velocity. After 10 seconds, the two cells have endpoint alignment. The endpoint forces we apply succeed in creating endpoint alignment for two cells with the same orientation. **B** Two cells with opposite orientations and velocities of zero create endpoint alignment, demonstrating that our force succeeds in creating our desired alignment.

3.1.2 Two Cell Scenario with Opposite Orientations

To complete the two cell scenarios with the cells having nearly parallel orientations, we consider two cell scenarios with opposite orientations. Note that we can make the assumption that the two cells are nearly parallel in the general cases because of the cell-cell repulsion that aligns the cells in high density and creates the rafts we see in experiments. The repulsion force between overlapping cells greatly exceeds the force from the cell to continue in the direction of its orientation. Therefore, the repulsion forces almost always prevent cells from overlapping, causing alignment among cells. With greater cell density, the cells align themselves, meaning that our force does not need to align the cells to become nearly parallel.

Our new method of creating $\mathbf{F}_{\text{cell-cell}}$ succeeds in generating endpoint alignment among

two cells with opposite orientations and low velocities, which can be seen in Figure 6B as the cells align. These oppositely oriented cells must have a small enough velocity to align, or they will just move away from each other.

3.1.3 Two Cell Scenario with Non-Parallel Orientations

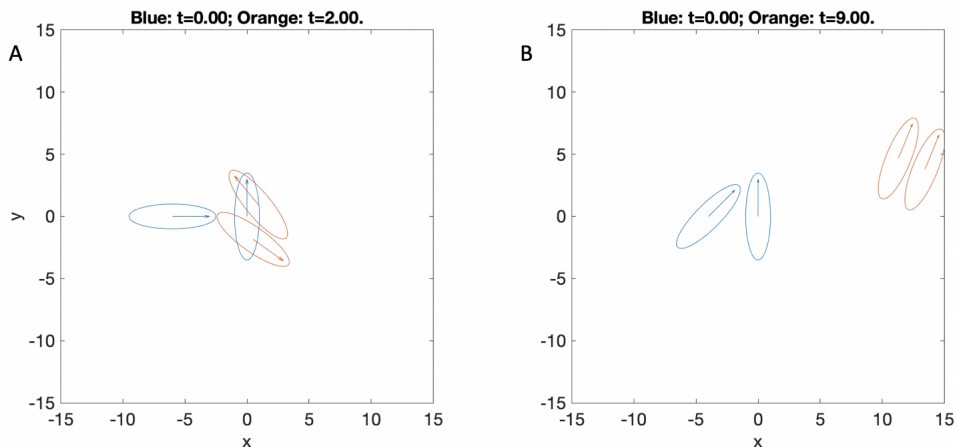


Figure 7: **A** We consider a two cell scenario with the two cells with perpendicular orientations. After $t = 2$, they are nearly parallel, with almost opposite orientations, so our endpoint interaction force combined with the cell-cell repulsion force creates nearly parallel orientation. **B** We consider when the two cells begin at a 45 degree angle. They are aligned at $t = 9$, so our model also succeeds in demonstrating that for two cells angled towards each other, they create near parallel orientation.

We now consider the scenarios in which the two cells are not parallel. In Figure 7, we consider scenarios in which the two cells begin at perpendicular and non-parallel orientations. They quickly move to become nearly parallel by cell-cell repulsion forces and by $\mathbf{F}_{\text{cell-cell}}$. These two simulations validate our previous assumption that the two cells could be assumed to be parallel or nearly parallel.

3.2 Multi-Cell Scenario with Parallel Orientation

We continue to study scenarios with more cells using our new model. We first consider a scenario with 10 cells, all with the same orientation and evenly spaced. If their velocities are all the same, then no matter the length of these cells, they will all form endpoint alignment and move together with the same speed with the endpoint alignment as seen in Figure 8.

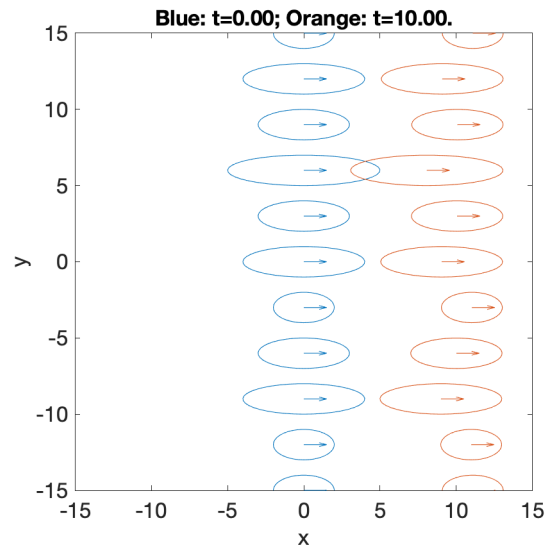


Figure 8: Even with different length cells, the cells still align if they have the same speed, are evenly spaced, and have orientational alignment. We can see that for 10 cells, they align with endpoint alignment.

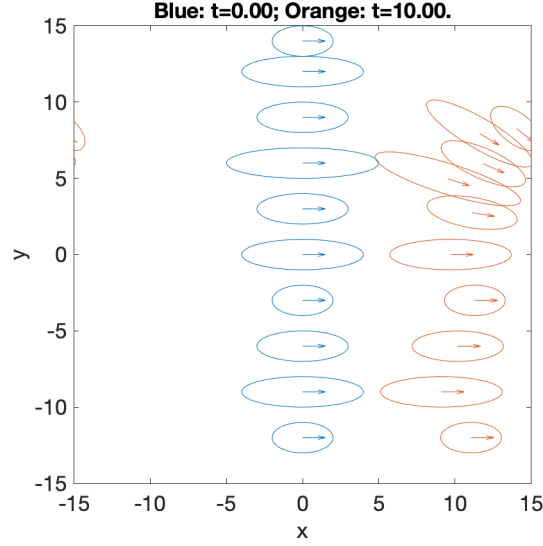


Figure 9: In this scenario, the cells all have the same speed and orientation. However, when they are not evenly spaced, they do not create a linear endpoint alignment as seen in Figure 8. They form a curved endpoint alignment.

However, if these cells are not evenly spaced, they will not create endpoint alignment in the same manner. Even with the same starting orientations and speeds, the cells will create smaller rafts as seen in Figure 9. When the cells at the top of Figure 9 approach each other, the $\mathbf{F}_{\text{cell-cell}}$ and repulsion forces both work against each other, leading to a small raft of three cells at the top of our simulation. The small raft of three cells then moves into the other aligned cells, creating a curved endpoint alignment among the cells due to the endpoint interaction force and cell-cell repulsion forces. Although this simulation does not create linear endpoint alignment, the curved endpoint alignment demonstrates that our model still creates endpoint alignment among cells.

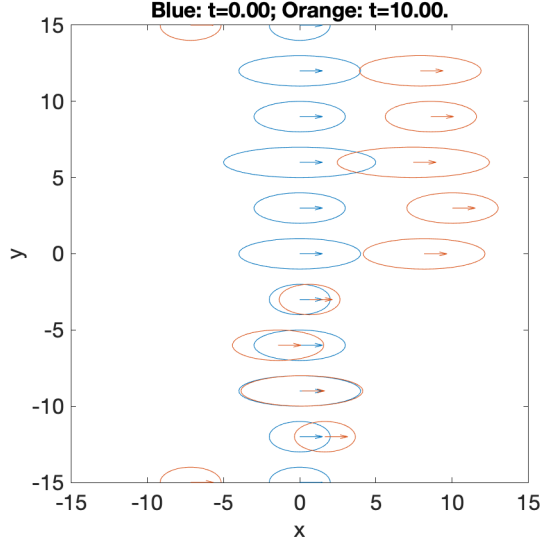


Figure 10: When the cells have varying lengths and velocities, they will naturally form their own rafts, with a higher speed raft and a lower speed raft. Here the upper five cells have a greater speed than the lower five cells, and they form their own raft. The cells in these rafts drag each other to maintain alignment.

When we simulate a scenario with 10 cells with the same orientation but different lengths and velocities, we notice that the cells with greater velocity form their own rafts in front of the cells with lower velocity. We can see that in Figure 10 the cells with greater velocity will form their own raft naturally. This demonstrates that our model not only works for two cell scenarios but also naturally creates rafts just as they occur in experimental observations.

When the cells are not moving toward the same orientation, they do not create endpoint alignment as the cells in Figure 8 and do not create rafts as the cells in Figure 10. We study two scenarios of cells with opposite orientations. In Figure 11A, the cells have alternating orientations, with every other cell having opposite orientations. In Figure 11B, the upper five cells have orientation leftward, while the lower five cells have orientation rightward. We observe that the upper five cells remain close to each other, while the lower five cells also remain close to each other. Neither raft forms smectic alignment, but they tend to form their own rafts naturally. The formation of these two rafts demonstrates that our model succeeds in simulating the scenario, as these raft formations occur naturally in our model and in

experiments as well.

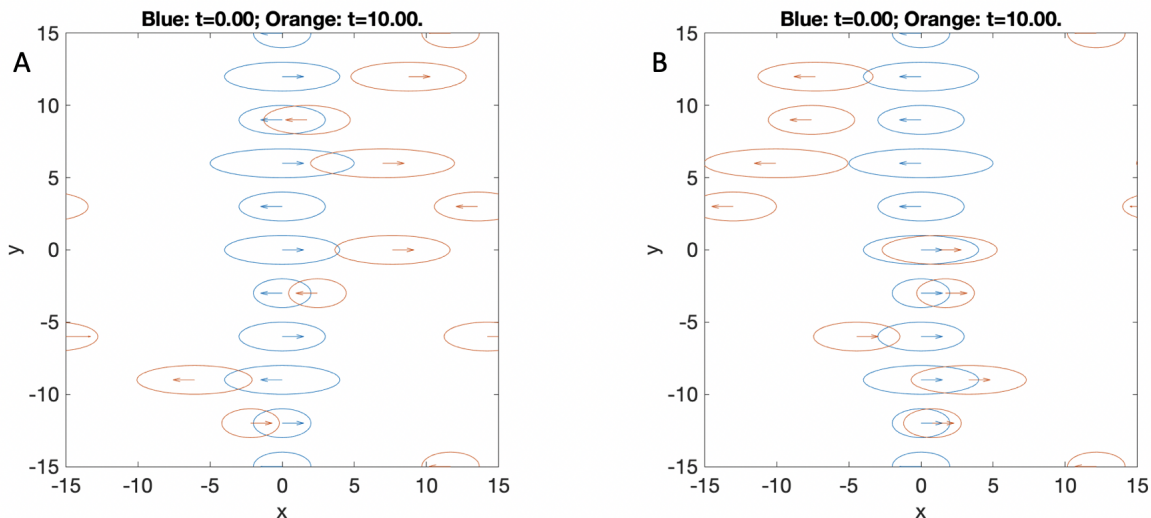
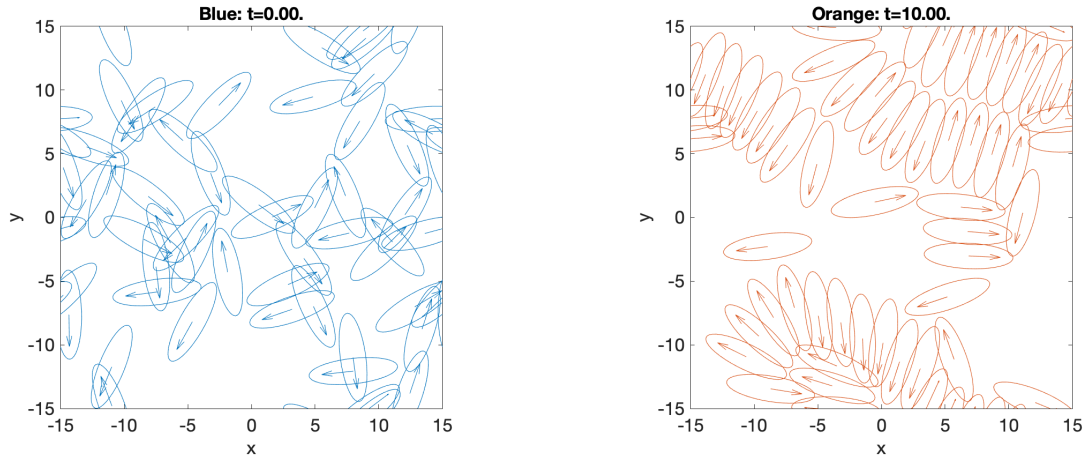


Figure 11: **A** The alternating cells have opposite orientations. They do not form rafts or endpoint alignments because the cells which have the same orientation are not close enough to each other to create rafts. **B** The top five cells and the bottom five cells have different orientations, and we note that the cells with the same orientation form separate rafts. The cells with the same orientation are close enough to form rafts in this scenario.

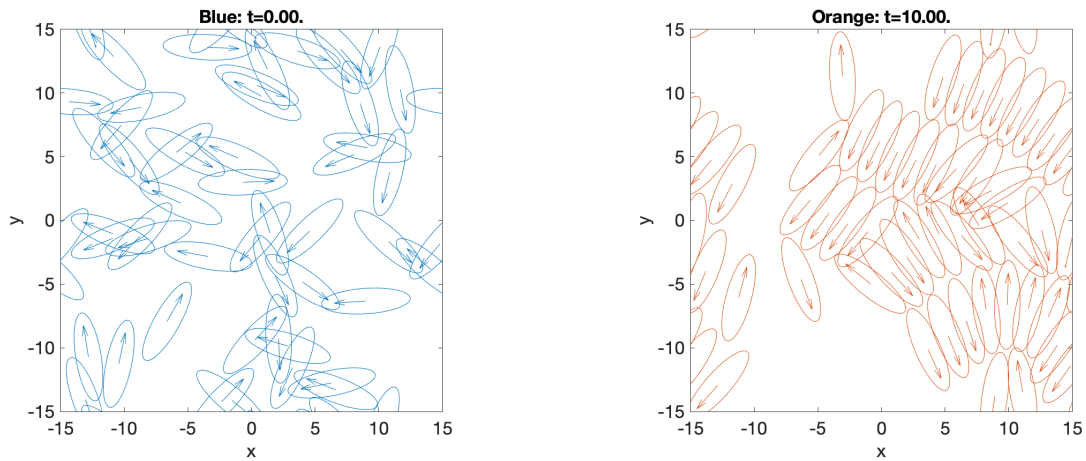
3.3 Multi-Cell Scenario with Random Positions and Orientations

We now study scenarios with 50 cells with random alignments and random positions to examine if our added $\mathbf{F}_{\text{cell-cell}}$ creates endpoint alignment within the simulation. We assign random \mathbf{x}_α and $\hat{\mathbf{n}}_\alpha$ to each cell α . Each cell has the same velocity and half-length. We test three different simulations, as seen in Figures 12, 13, and 14, of the same scenario with random positions and random orientations to determine if any clear patterns exist.



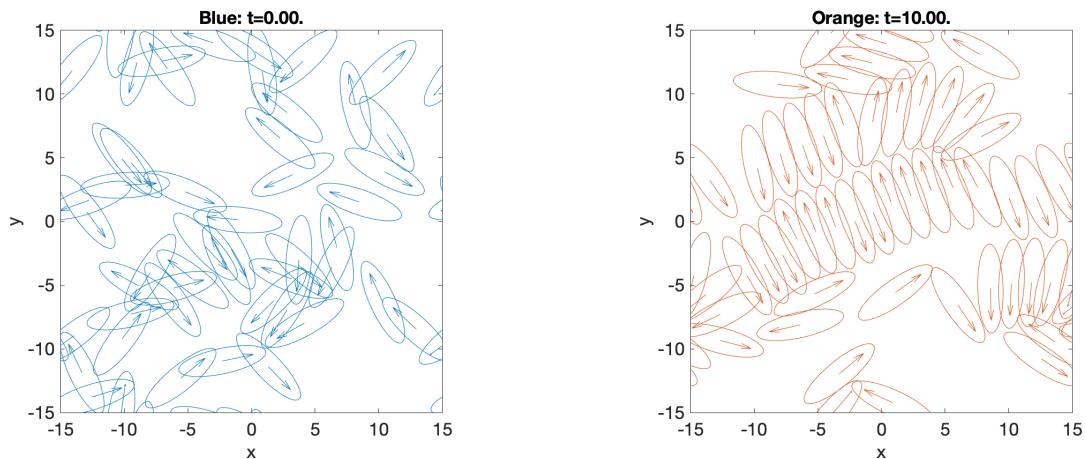
(a) Initial configuration of the 50 cells in random positions with random orientations (b) 50 cells after the endpoint interaction forces and cell-cell repulsion forces act on them for $t=10$

Figure 12: First fifty cell simulation with random positions and random orientations. We observe both curved and linear endpoint alignment, demonstrating that our model succeeds in creating endpoint alignment.



(a) Initial configuration of the 50 cells in random positions with random orientations (b) 50 cells after the endpoint interaction forces and cell-cell repulsion forces act on them for $t=10$

Figure 13: Second fifty cell simulation with random positions and random orientations. We observe both curved and linear endpoint alignment, demonstrating that our model succeeds in creating endpoint alignment.



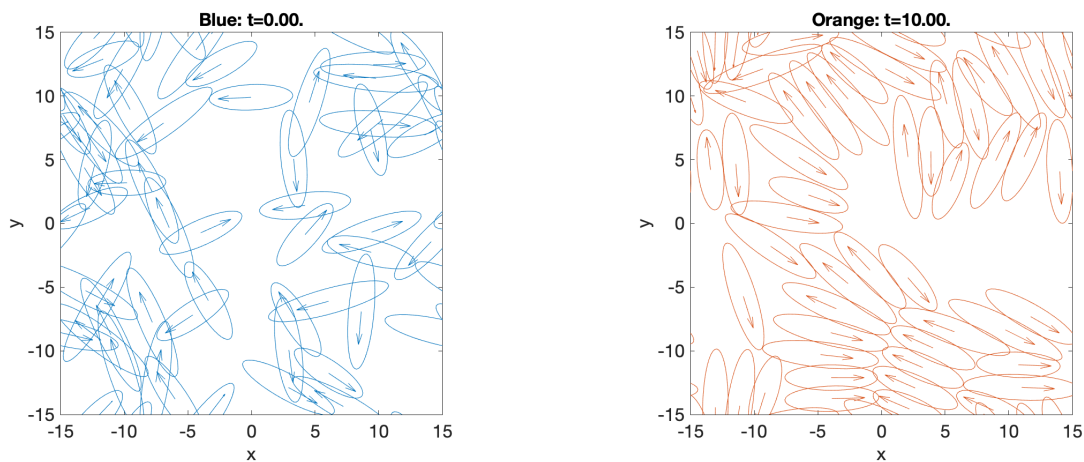
(a) Initial configuration of the 50 cells in random positions with random orientations (b) 50 cells after the endpoint interaction forces and cell-cell repulsion forces act on them for $t=10$

Figure 14: Third fifty cell simulation with random positions and random orientations. We observe both curved and linear endpoint alignment, demonstrating that our model succeeds in creating endpoint alignment.

We observe the fifty cell simulation with random orientations and random positions. After $t=10$, we notice smectic alignment on the upper left side and upper right side of Figure 12b. On the bottom of Figure 12b, we notice a raft, with a curved endpoint alignment. In Figure 13b, we see three rows of smectic alignment in the upper right corner with a slanted endpoint alignment. Because the cells are all the same length, the endpoint interaction force creates endpoint alignment throughout the right side of the figure. We see a curved endpoint alignment in the lower left area of Figure 13b. This demonstrates that the cells do not all form linear endpoint alignment that our model hopes to achieve, but some form curved alignments which remain in equilibrium due to the balanced cell-cell repulsion forces and endpoint interaction forces. We notice a linear smectic alignment through the middle of Figure 14b. There is also a curved endpoint alignment on the lower left side of Figure 14b. Even with the random orientations and random positions, we notice that the cells do form their own rafts with endpoint alignments, as some have linear endpoint alignments and some have curved endpoint alignments.

These simulations support our model, as the randomly oriented cells form linear and curved endpoint alignments in their rafts. We observe these patterns largely due to our endpoint interaction force that we added as well as the cell-cell repulsion force. When many cells crowd an area, the endpoint interaction forces increase, sometimes even overcoming the cell-cell repulsion forces to create configurations in which the cells appear to be overlapping. Our model was designed to create linear endpoint alignment, as the endpoint interaction force becomes zero when the two cells endpoints line up perpendicular to the orientation. Although our model was not designed for curved endpoint alignment, the endpoint interaction force balances with the cell-cell repulsion forces to create an equilibrium where the cell alignment is curved.

We now test a simulation with cells of varying lengths. We choose our lengths to have a random length from 3 to 5 based on experimental evidence.



(a) Initial configuration of the 50 cells in random positions with random orientations (b) 50 cells after the endpoint interaction forces and cell-cell repulsion forces act on them for $t=10$

Figure 15: Fifty cell simulation with random lengths, random positions, and random orientations.

We notice that the simulation with uneven lengths in Figure 15b demonstrates endpoint alignment just like the previous simulations with the same length cells. We see smectic alignment in the lower raft of cells across the bottom of the simulation. We notice some

nematic alignment along the top of the simulation, with curved endpoint alignment on the upper right side of the simulation. Our model does not create as much smectic alignment as we would expect because of the different lengths of the cells. When smaller cells align with larger cells, they create endpoint alignment on one end, but they do not on the other end. This misalignment leads to further nematic alignment rather than smectic alignment throughout the simulation, which can be seen in Figure 15b.

4 Conclusion

In our study, we use MATLAB to test our model and simulate cell-cell interactions. We study 2 cell scenarios, 10 cell scenarios, and 50 cell scenarios. In our 2 cell scenarios, we test our model with orientationally aligned cells in Section 3.1.1, oppositely oriented cells in Section 3.1.2, and non-parallel cells in Section 3.1.3. In our 10 cell simulations in Section 3.2, we test when the cells are all parallel. We simulate five different scenarios in which we change the orientation, speeds, and locations of the 10 cells. In our 50 cell scenarios in Section 3.3, we create random positions and orientations for the cells while also using random cell half-lengths in one simulation.

In our 2 cell scenario, we test the model with orientationally aligned cells. The model succeeds in creating endpoint alignment between the two cells even with different length cells and different speeds. The endpoint interaction force creates the endpoint alignment, as the faster cell drags the slower cell to maintain the alignment. When the two cells are oppositely oriented, they just move away from each other in the direction of their orientation unless the velocity of both cells is close to zero. We then test to determine if we can assume that the cells are close to parallel in the general scenarios. We simulate two scenarios in which the two cells are perpendicular and are slanted towards each other. In both scenarios, the cells create their own alignment as seen in Figure 7.

In our 10 cell scenarios, we notice that when the cells are orientationally aligned and have the same speed, they create endpoint alignment if they are evenly spaced. If they are not evenly spaced, the cells form a curved endpoint alignment. When the cells have varying speeds and are orientationally aligned, the cells with greater speeds naturally form their own raft, while the cells with lower speeds form their own raft.

In our 50 cell scenarios, when the cells are randomly oriented and have random positions with the same half-lengths, we notice linear and curved endpoint alignment. Despite the random orientations and positions, our added endpoint interaction force in the model serves to help create more smectic alignment than nematic alignment. For the scenario with random cell lengths as well as random orientations and positions, the simulation still demonstrated smectic and nematic alignments throughout the system.

5 Future Work

As future work, we would like to consider a more general equation which includes cases in which the two cells are not aligned. Although our equations work for nearly parallel cell scenarios, we would like to extend the equation to include some special configurations in which the two cells are not parallel with each other. We would also like to consider the three-dimensional case of creating endpoint alignments with biofilms. The model would be different from our current model, as biofilms were previously analyzed by Hartmann et al. [4]. This scenario would provide unique challenges not found in our two-dimensional study. We also would hope to write the code for our simulation in a different language which would allow us to run simulations with more cells. In MATLAB, we can only practically run simulations with less than 100 cells. With some other language, we would be able to create a large-scale simulation to more accurately represent our model and the cell interactions. We would prefer to be able to create simulations in reasonable times with much more cells than our 100 cell

limit. We would be able to study higher cell density scenarios, which occur naturally in experiments.

6 Acknowledgments

I would like to thank Boya Song for her help writing the code and guiding my simulations throughout this entire research process as my mentor. I would also like to thank Dr. Tanya Khovanova for her guidance and advice on the paper as the head mentor. I would like to thank Professor David Jerison and Professor Ankur Moitra for their help with my presentation and project idea. I would also like to thank Dr. John Rickert for his constant help on my paper and advice for my presentation. I would like to thank Sean Elliott for providing great feedback on my paper. I would like to thank the Massachusetts Institute of Technology Mathematics Department for allowing me to perform research in their facilities and the Massachusetts Institute of Technology for allowing me to stay on their campus. I would like to thank Jane Street Capital, James C. Ellenbogen, Mr. and Mrs. George Eltringham, and Mr. Songrong Hou and Ms. Hongbing Chen for sponsoring my stay at the Research Science Institute. I would like to thank the Center for Excellence in Education, the Research Science Institute, and the Massachusetts Institute of Technology for providing me with this opportunity to perform research.

References

- [1] H. Jeckel, E. Jelli, R. Hartmann, P. K. Singh, R. Mok, J. F. Tetz, L. Vidakovic, B. Eckhardt, J. Dunkel, and K. Drescher. Learning the space-time phase diagram of bacterial swarm expansion. *Proceedings of the National Academy of Sciences*, 116(5):1489–1494, 2019.
- [2] L. L. Burrows. *Pseudomonas aeruginosa* twitching motility: Type iv pili in action. *Annual Review of Microbiology*, 66(1):493–520, 2012.
- [3] Libretexts. 11.8: Liquid crystals. [https://chem.libretexts.org/Bookshelves/General_Chemistry/Map:_Chemistry_\(Averill_and_Eldredge\)/11:_Liquids/11.8:_Liquid_Crystals](https://chem.libretexts.org/Bookshelves/General_Chemistry/Map:_Chemistry_(Averill_and_Eldredge)/11:_Liquids/11.8:_Liquid_Crystals), Jun 2019.
- [4] R. Hartmann, P. K. Singh, P. Pearce, R. Mok, B. Song, F. Díaz-Pascual, J. Dunkel, and K. Drescher. Emergence of three-dimensional order and structure in growing biofilms. *Nature physics*, 15(3):251, 2019.